Final version at http://ecst.ecsdl.org/content/61/7/11.abstract

Carbon-electrode Dielectrophoresis for Bioparticle Manipulation

R. Martinez-Duarte

Department of Mechanical Engineering, Clemson University,
Clemson, South Carolina 29634, USA

This work presents the latest application of carbon-electrode Dielectrophoresis, a technique for particle separation. The use of 3D carbon electrodes allows for higher throughput and efficiency when compared to more traditional DEP techniques, such as metal-electrode and insulator-based DEP. The applications presented here all feature a protocol that allows for enrichment and purification of a targeted particle population from a sample; and effectively enables sample preparation for downstream analysis. The final goal is the integration of independent carbon-electrode arrays, optimized in their geometry and polarizing signals, to achieve an automated sample preparation device comprising functions such as concentration, purification and lysis.

Introduction

Dielectrophoresis (DEP) is a field-based technique enabling the selective manipulation of a targeted particle, or population of particles,using the interaction of a non uniform electric field with the induced effective dipole moment of the targeted particle(s). DEPis advantageous over other particle separation techniques such as flow cytometry or FACS (Fluorescence-activated cell sorting) and magnetophoresis or MACS® (Magnetic-activated cell sorting) because discrimination between different particles is based solely on their intrinsic physical properties, such as surface structure and internal compartmentalization; and not on external tags like antibody-linked fluorophores or magnetic nanoparticles. Such physical properties will determine the particle's dielectric properties and give it a characteristic dielectric phenotype. DEP has been demonstrated in a variety of applications, ranging from the manipulation of cells and bacteria, to the separation of proteins and other molecules.

One of the requirements to induce a DEP force on a sample is the creation of a non uniform electric field to create volumes of different field magnitudes across the sample. A number of techniques have been developed to establish such field gradient throughout a sample and the reader is directed to the recent extensive review on such techniques by Martinez-Duarte (1). The work being presented here pertains to the use of carbon electrodes to induce a DEP force, in a technique now known as carbon-electrode Dielectrophoresis, or carbonDEP. Glass-like carbon electrodes are derived through the pyrolysis of photo patterned epoxy following a fabrication technique known as CarbonMEMS.

The use of carbon electrodes yields some key benefits that make carbon-DEP an advantageous alternative to other well-established DEP techniques, such as metal-

electrode based DEP or insulator-based dielectrophoresis (iDEP). For example, carbon has a much wider electrochemical stability window than metals commonly used in metal-electrode DEP, such as gold and platinum, and therefore affords higher applied voltages, and higher field magnitudes, in a given solution without electrolyzing it (2). Even though the electrical conductivity of glass-like carbon (3, 4) is lower than that of metals, suitable electric fields for DEP can be generated by polarizing carbon electrodes with voltages in the range of tens of volts instead of the hundreds of volts required in other DEP techniques using insulating structures, namely iDEP, to locally distort an otherwise external and uniform electric field. The use of carbon electrodes yields other advantages such as excellent biocompatibility (5, 6), 2) remarkable chemical inertness in almost all solvents/electrolytes (7, 8) and 3) excellent mechanical properties (9, 10).

Furthemore, the use of 3D structures that cover the entire height of a flow channel will be presented as an enabling improvement towards more practical applications for DEP. The use of such structures greatly improves throughput and efficiency of DEP devices by reducing the mean distance of any particle to the closest electrode surface. This is in contrast to the performance achieved when using more traditional 2D (planar) electrodes positioned at the bottom of a flow channel where many targeted particles immersed in the bulk volume of the channel do not come close to the electrical field gradient surrounding the planar electrodes and are not influeced by a DEP force. After a brief introduction to both the general theory behind DEP and the process used to fabricate 3D carbonDEP devices, the reader will be presented with the latest applications of 3D carbonDEP. Other applications of carbonDEP can be found elsewhere (11-13), including the integration of carbonDEP devices with centrifugal microfluidics.

Theoretical Background

The basic DEP equations are provided in this section, with the main purpose of introducing the reader to the concepts of positive and negative DEP. The reader may find further details on the theory behind DEP in the works by other authors (14, 15). The DEP force induced on a particle depends on the magnitude and non-uniformity of an externally applied electric field, as well as the relation between the physical and electrical parameters, such as conductivity and permeability, of the surrounding medium and the targeted cell, as described in Equation 1:

$$F_{DEP}=2\varepsilon_m r^3 \mathrm{Re}[f_{CM}]\nabla E_{rms}^2 \quad [1]$$

where r is the radius of the cell, E_{rms} the root mean square of the electric field (which is related to the geometry of the electrodes polarizing the sample), ε_m the permittivity of the medium, and $\mathrm{Re}[f_{CM}]$ the real part of the Clausius-Mossotti factor (f_{CM}) defined as

$$\mathrm{Re}[f_{CM}]= (\varepsilon_p^* - \varepsilon_m^*) / (\varepsilon_p^* + 2\varepsilon_m^*) \quad [2]$$

With ε_p^* being the complex permittivity of the particle, and ε_m^* that of the medium. Complex permittivity ε^* is given by

$$\varepsilon^* = \varepsilon - j\sigma/2\pi f \quad [3]$$

and depends on the permittivity ε and conductivity σ of the cell or the medium and the frequency *f* of the applied electric field. *j* represents the imaginary number -1. A positive sign of Re[f_{CM}], known as positiveDEP or pDEP, denotes a DEP force that causes cells to migrate up the field gradient, or to those regions of high field strength. Negative values of Re[f_{CM}] denote the opposite behavior, cells moving toward regions of low or no field strength, and accordingly is designated negative dielectrophoresis (nDEP). A pDEP or nDEP behavior depends on the difference on polarizability between the targeted bioparticle and its surrounding media. A positive DEP force on a particle arises when the complex permittivity of the targeted particle is higher than that of the suspending medium. A negative DEP force is present otherwise. As stated in equation 3, complex permittivity depends on the frequency of the electric field and a particle may be influenced by pDEP forces at one frequency but under nDEP force at another frequency value, even when the suspending media remains the same. For example, latex particles are shown in figure 1A selectively confined to nDEP regions, those furthest away from the electrode surface, using a polarizing signal of frequency 10 MHz. *M. smegmatis* bacterial cells are shown both under nDEP in figure 1B and under pDEP in figure 1C; one can switch from negative to positive DEP behavior by changing the frequency from 100 kHz to 7 MHz. The magnitude of the signal is 20 V_{pp} in all cases. No flow was established in any of these experiments. It is clear that one can optimize the frequency, magnitude and medium conductivity to achieve a specific DEP regime for targeted particles.

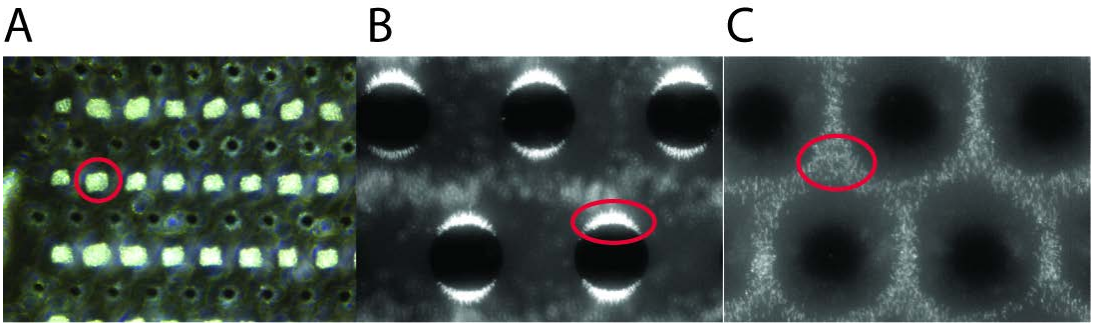

Figure 1. Particle positioning shown in red ellipses: A) Latex particles (8 um diameter) under nDEP, B) *M. smegmatis* under nDEP and C) pDEP.

Device fabrication

The complete fabrication process is illustrated in figure 2 and has been detailed elsewhere (16). The process starts with the photo-patterning of a carbon precursor on a suitable substrate. Carbonization is usually performed at 900 °C, and thus viable substrates will include refractory materials such as silicon, silicon oxide or fused silica. Other substrates like sapphire may also be used but their cost may limit their application. SU-8, an epoxy-based negative photoresist has been used extensively by this author as the carbon precursor. SU-8 photolithography is implemented in two steps: 1) fabrication of planar interdigitated fingers that will become carbon connection leads to the base of the 3D carbon electrodes and 2) fabrication of SU-8 pillars that will become the 3D

carbon electrodes. Details on the process parameters to fabricate selected SU-8 structures on silicon and fused silica substrates can be found in (16) and (17) respectively.

The carbonization process features an inert atmosphere, usually nitrogen, and comprises 2 heating stages: 1) a temperature ramp from room temperature to 200 °C at 10 °C·min^{-1} followed by a 30 minute dwell at 200 °C, to allow for any residual oxygen to be evacuated from the chamber and prevent combustion of the polymer as the temperature is raised further; and 2) a temperature ramp from 200 to 900 °C at 10 °C·min^{-1} with a one-hour dwell at 900 °C to complete a 95-99% carbonization of the epoxy precursor. The samples are then cooled down to room temperature at a ramp of 10 °C·min^{-1}. Near-isometric shrinkage occurs during pyrolysis and is detailed elsewhere (16). After pyrolysis, the carbon electrodes and the areas in between are de-scummed using oxygen plasma to eliminate any carbon residues between the electrodes that could lead to an electrical short-circuit during experiments. A thin layer, ~2 μm, of SU-8 is then patterned around the carbon electrodes to electrically insulate the connection leads and to planarize the surface around the base of the electrodes.

The microfluidic network is fabricated separate from the carbon electrodes. The network is fabricated out of pressure-sensitive double-sided adhesive (PSA) and polycarbonate (PC). A microchannel is first cut from an adhesive laminate using a cutter-plotter and is aligned to the channel inlet and outlet, which had been previously drilled in a PC substrate. The carbon electrode array is then manually aligned with the PSA-PC stack such that the electrode array is contained inside the microfluidic channel. Experimental devices are then sealed using a rolling laminator. Inlet and outlet ports to and from the channel are implemented using commercial connectors, such as NanoPort™ from IDEX Upchurch Scientific, or connectors fabricated in-house.

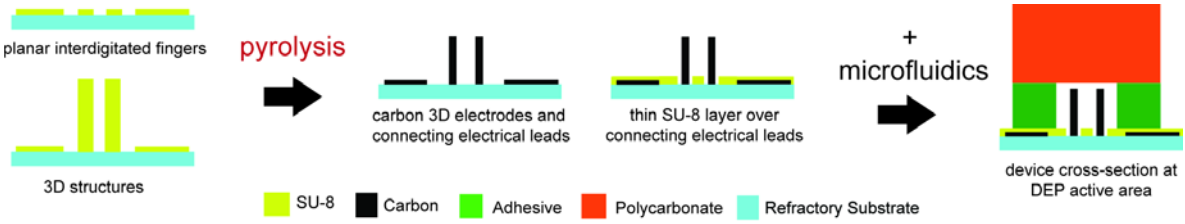

Figure 2. Fabrication of carbon electrodes, see details in the text.

Applications

In this section, I will detail the latest application of 3D carbonDEP as an active filter for the trapping and purification of selected particles. All these applications are based on a similar experimental protocol, which features three main stages: 1) extract targeted particles from the sample by trapping them on the electrode array using pDEP; 2) hold the particles on the electrode array by pDEP forces while a washing solution is flowed through the channel; and 3) release the targeted particles, by de-polarizing the electrode array, for collection at the exit of the channel. In such way, one can enrich and purify a selected particle population from a given sample. Three applications are presented next: a) elimination of natural contaminants to increase sensitivity of PCR-based protocols, b)

enrichment of bacterial persisters from an antibiotic-treated sample; and c) trapping of lambda DNA, towards future protocols for enriching biomolecules in diagnostic applications.

Increasing the sensitivity of PCR-based protocols. Both PCR and real-time PCR are nowadays the methods of choice for the rapid analysis of several types of biological samples. Although several PCR protocols have been optimized to increase sensitivity, the current challenge is to eliminate inhibitors of polymerase that may be present in the biological/environmental sample and that may interfere with PCR such as bile salts in faeces, heavy metals and humic substances in soil, collagen in food samples, heme in blood, phenolic compounds, and proteinases in milk (18-20). In many instances, protocols for DNA extraction from complex environmental samples cannot completely prevent co-extraction of PCR-inhibiting compounds (21) and approaches to overcome PCR failure due to inhibitors present in the sample are constantly being developed. Unfortunately, the list of inhibitory substances is rather large. Reported strategies to overcome PCR inhibition include sample-washing steps, density gradient centrifugation, gel electrophoresis, column chromatography and even the use of additives such as bovine serum albumin (19, 22). However, these methods tend to be cumbersome, time demanding and often expensive. In spite of the wide variety of approaches reported, interference of the sample with PCR is still a major concern when analyzing several types of samples.

3D carbonDEP is presented here as a viable alternative to prepare samples prior to PCR processing. The aim was to demonstrate the practical use of DEP as a lab-based sample preparation tool which can significantly improve the sensitivity of PCR analysis, not only with cells cultured in conventional growth media, but with natural samples as well. The full details of these experiments have been published elsewhere by this author and his collaborators (23). The samples used in such work all featured *S. cerevisiae* cells, grown following standard protocols, but re-suspended in different media: 1) Sabouraud broth; 2) fermented grape must and 3) different concentrations of humic acids. Here I will omit the results obtained using fermented grape must and focus on those obtained when working with humic acids since they are the most prevalent PCR inhibitors in soils and natural surface waters (20, 24). Sabouraud broth is known to not interfere with PCR analysis. The limit of detection of yeast cells depending on the concentration of humic acids in the sample was first determined using only PCR. The results were then compared to the limit of detection of yeast cells in samples with increasing concentration of humic acids, but this time using PCR complemented with carbonDEP-based sample preparation. The goal was to demonstrate that the sensitivity to *S. cerevisiae* cells achievable by PCR in a sample containing humic acids could be increased by trapping, washing and re-suspending yeast cells in a PCR inhibitor-free media, *i.e.* Sabouraud broth, using 3D carbonDEP.

If present in the sample, humic acids appear to be able to form complexes with the extracted DNA. Such complexes are not easily separable and can thus easily mask the presence of targeted DNA. The importance of this work was the removal of humic acids from a sample, an important step that could enable PCR detection of targeted organisms in an environmental sample. The first step was to assess the minimal concentration of humic acids that inhibits PCR detection of yeast cells. To this end, an overnight culture of *S. cerevisiae* cells in Sabouraud broth was split into fractions and supplemented with

humic acids in a concentration range from 1 to 100 µg/ml. Samples were then PCR-analyzed to detect *S. cerevisiae* cells. The maximal concentration of humic acids that still allowed for detection of yeast cells was 10 µg/ml as shown in Fig. 3A. The reader is reminded that Seboraud broth does not interfere with PCR analysis. In order to verify the capability of the carbon-DEP chip to remove humic acids from a sample and increase the sensitivity of the PCR protocol as used before, an overnight culture of *S. cerevisiae* in Sabouraud broth was first diluted with DI water and then fractioned into seven 1 ml. samples. Humic acids were added to each of them in a concentration ranging from 10 to 100 µg/ml. Fractions of each of these seven samples, 200 ul, were independently subjected to a DEP-based sample preparation protocol where such fractions were flowed, at 20 ul/min, through a polarized electrode array, at 5 MHz and 10 V_{pp}, to trap viable yeast cells. The trapped cells were then washed with clean Sabouraud media for 30 minutes and finally released for retrieval at the channel exit by turning the field off. 9.8 ul from the first eluate retrieved from the chip after the field is off were then mixed with 0.2 ul of NaOH 1M and PCR-analyzed to detect yeast cells. The results obtained for each of the seven samples are shown in Fig. 3B and evidence that humic acid concentrations up to 75 µg/ml can be removed by implementing a DEP-based enrichment and purification step before PCR analysis. Therefore, high-throughput 3D carbonDEP chips can be used as pre-PCR sample processing strategy to purify a population of microorganisms and significantly improve the detection sensitivity of PCR. In less than 30 minutes, precise numbers of cells could be extracted from a sample volume of 200 ul, washed and eluted in reduced volumes which are appropriate for PCR analysis. Humic acids, important PCR inhibitors, were readily washed out.

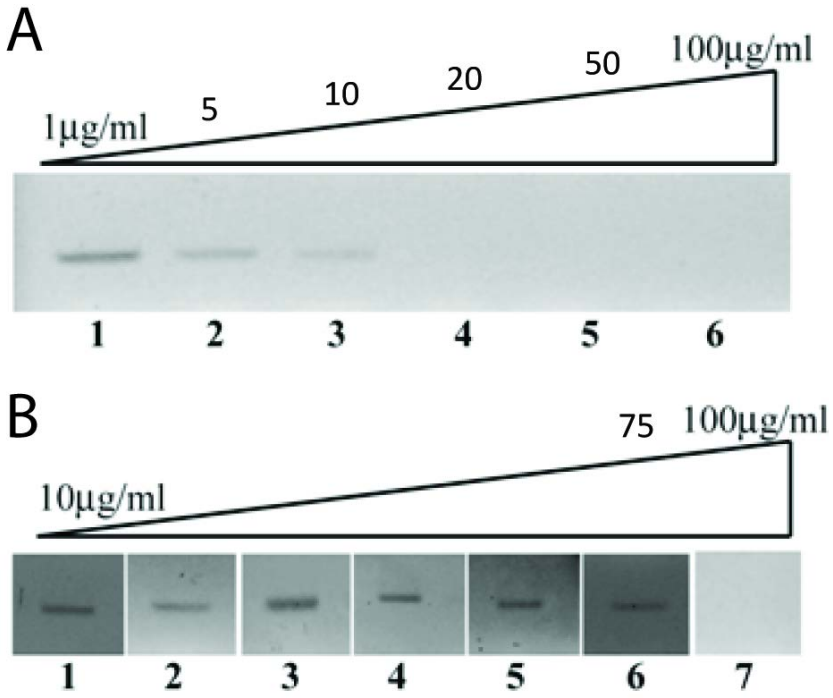

Figure 3. PCR results demonstrating A) the inability of only PCR analysis to clearly detect yeast cells when the concentration of humic acids in the sample is above 10 ug/ml and B) significant improvement obtained when using a carbonDEP-based sample preparation module before PCR analysis: humic acids concentrations up to 75 ug/ml are effectively removed from the sample to enable yeast detection. From (23).

Enriching bacterial persisters after antibiotic treatment. Bacterial persistence, first described by Bigger in 1944 (25), has been observed in many different bacterial species exposed to different classes of antimicrobials. Bacterial persistence is a clinically important problem, as it is thought to be responsible for treatment failures, post-therapy relapses, and lengthy treatment regimens in diseases such as leprosy and tuberculosis. Despite this, there have not been many studies to characterize these persisters or to understand the mechanism of persistence, chiefly due to the following reasons. First, the fraction of persister cells is often very small (10^{-3} to 10^{-6} or lower), which complicates their analysis within mixed populations comprising persister (minority) and non-persister (majority) subpopulations. Second, the persister phenotype is not mediated through genetic changes and therefore is non-heritable. Instead, the phenotype is transient, usually lasting only as long as the drug remains in the environment. This makes it difficult to purify or isolate the tolerant subpopulations for further analysis. Third, since the persister fraction is usually a small fraction of the total population, analysis of this subpopulation is often confounded by contaminating signals from the majority non-persister dead cells or cell debris. Besides making it difficult to treat infections, the persistence phenomenon may also increase the probability of emergence of genetic resistance, thus contributing to the short lifespan of antibiotics after they reach the market. Therefore, there is a pressing need for new experimental tools to address the phenomenon of bacterial persistence. A better characterization of the persister sub-population could enable the design of new drugs that target the persister population and help in reducing the duration of treatment of recalcitrant infections (26, 27). Purification would facilitate the characterization of these subpopulations using conventional ‘omics-based approaches (28, 29). While fluorescence-activated cell sorting (FACS) is the most common enrichment technique and provides high-throughput fractionation of cell populations, this technique requires cells to be differentially labeled, which could potentially change the phenotype of the organism.

3D carbonDEP was used for the isolation and purification of bacterial cells remaining viable after a 24-hour treatment with isoniazid (INH), a frontline anti-tuberculosis drug. *M. smegmatis* was used in this work as a model organism to investigate mechanisms of dormancy or drug-cell interactions in mycobacterial infections, such as tuberculosis. In a proof-of-concept study this author and his collaborators demonstrated label-free isolation and enrichment of viable bacterial cells, deemed persisters, in sufficient numbers for possible downstream analysis using conventional methods such as proteomic and transcriptomic analysis (30).

The results presented demonstrated DEP-based enrichment of intact *M. smegmatis* cells from a mixed input population of INH-treated cells comprising about 90% intact cells and 10% damaged cells. After following an experimental protocol similar to the one presented above, the intact cell population was enriched from 90 to up to 99% purity and recovered from the carbonDEP chip as shown in figure 4. The X-axis denotes the sequential fractions recovered from the chip. Trapping from the original sample (control) happens in fraction 1-4 and washing in fractions 5-9. The purified population is retrieved in fractions 10-15. Therefore, DEP-based purification of persister cells could provide a useful tool to provide an idealized sample to ‘omics-based analysis and shed more light into the mechanisms of persistence under INH exposure. Furthermore, most of the ‘omics based approaches for downstream characterization of purified bacterial populations

require a sample containing at least 10^5-10^6 targeted cells. As can be seen from Fig. 4, the established DEP protocol allowed for the recovery of up to $3X10^4$ intact cells, with up to 99% purity, per assay. Using this setup, serial assays could provide the user with enough material to perform downstream analysis. Current work is focused on increasing the trapping throughput of the system, up to 10^6 cells, by increasing the dimensions and number of electrodes in the carbonDEP array; and maximizing the electric field gradient magnitude throughout the array.

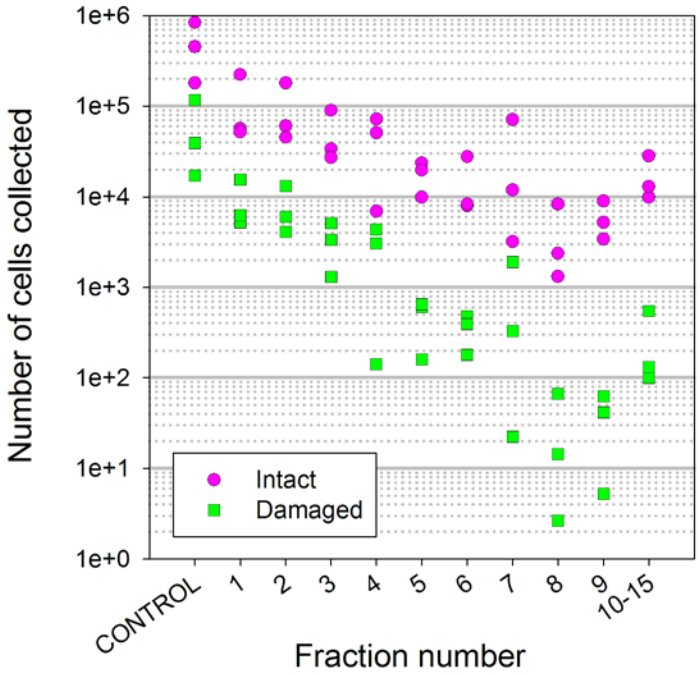

Figure 4. Intact and damaged cell counts (y-axis) of the sequential fractions recovered during the carbonDEP assay. The control fractions refers to the original sample, flowed through the chip without polarizing the electrode array. Green triangles represent viable cells while inverted red triangles represent non-viable cells. Symbols correspond to three representative experiments. From (30).

DNA concentration. The DEP behavior of DNA under the influence of an electric field gradient within a carbon electrode array has also been studied. Again, details of this work can be found on the work from this author and his collaborators (31). Similar carbon electrode geometries than those used in the previous two applications were used to trap YOYO-labeled λ-DNA. The goal of this work was two-fold: towards a tool to facilitate the study of DNA biophysics by studying the interaction of the hydrodynamic drag force and the DEP force; and to demonstrate the capability of carbonDEP to trap biomolecules. This last consideration is important towards the development of a carbonDEP-based sample preparation module capable of 1) purifying a targeted bioparticle population; 2) conduct electrical lysis on such population; and 3) concentrate the DNA and other internal organelles extracted during lysis. Lysis using a carbon electrode array has also been demonstrated recently by this author and his collaborators (32).

Figure 5A shows the experimentally observed DNA concentration around carbon electrodes upon application of an AC field. DNA concentration by pDEP was observed at frequencies between 10 and 50 kHz. However, it was concluded that a frequency of 10 kHz provides the most rapid and strongest concentration of DNA around the carbon electrodes. A 3D carbonDEP device was then used to implement an experimental protocol similar to that described above for the concentration and retrieval of λ-DNA. Figure 5B shows a characteristic elution profile for a 635 nM DNA solution with and without application of an electric field. The electrode array was polarized using a sinusoidal signal with a frequency of 10 kHz and magnitude of 16 V_{pp}. The flow rate in the channel was 2 µl/min. As in the case of the previous two applications, the elution profiles are divided into three phases: 1) 'sample', where the DNA is extracted from the solution and excess volume collected at the outlet; 2) 'washes', when pure buffer is flushed through the channel; and 3) 'eluates', indicating the potential polarizing the electrodes has been turned off causing the release of the targeted particle. Figure 5B demonstrates that DNA is retained in the carbon-electrode device and that, only after the potential was set to zero, a peak of higher DNA concentration is eluted. Such peak can clearly be distinguished from the flat baseline in the control experiment.

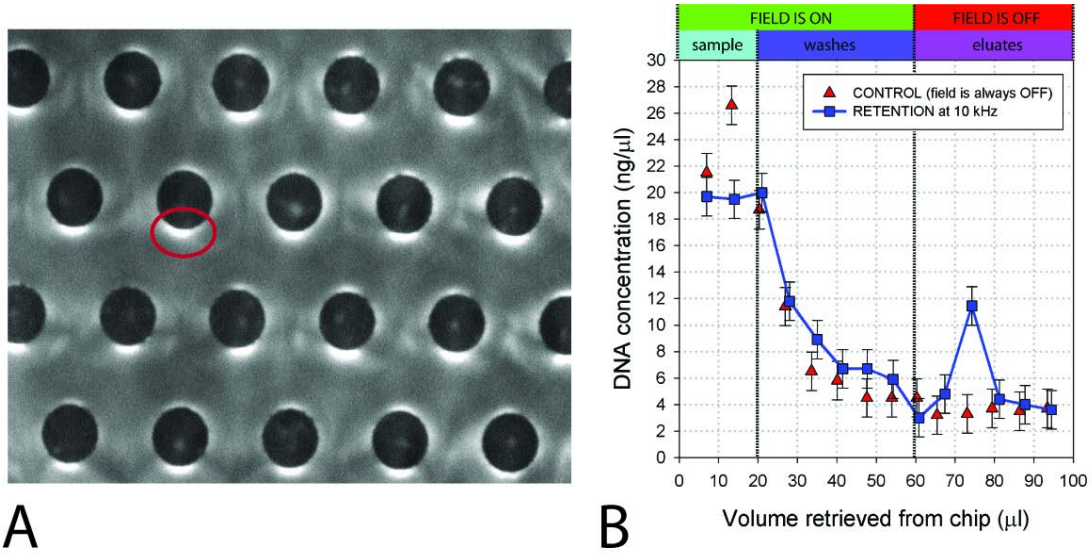

Figure 5. A) Fluorescence microscopy images showing DNA concentrated (red ellipse) on the surface of the electrodes by pDEP (AC signal featuring frequency of 10 kHz and magnitude 16 V_{pp}). B) Characteristic elution profile for a λ-DNA solution with and without the application of a DEP force. Note the characteristic peak obtained at volume equal 80 ul, right after the pDEP force is turned off and the previously trapped DNA is released. From (31).

Conclusion

The use of carbonDEP for three different applications has been briefly detailed. These applications included the trapping of *S. cerevisiae* yeast, *M. smegmatis* bacteria and λ-DNA. Advantages of the system reported in this work include high-throughput, efficiency and relative low cost. The 3D carbon-DEP chips are fabricated using fabrication techniques deemed low cost, namely photolithography, laminated object and drilling. The use of 3D electrodes, as tall as the channel and immersed in the bulk of the

sample, enables the addressing of all particles flowing in the channel leading to higher efficiency when trapping a targeted particle. Current work is on decreasing the cost of the devices, further increasing the throughput of carbonDEP devices and most importantly, the integration of electrically-independent electrode arrays in a single device towards automated sample preparation. A general schematic of a multi-stage device is presented in figure 6. A proof-of-concept has been described elsewhere (16, 33) and consists of different electrode array geometries sequentially positioned inside a microchannel. These array geometries can feature different electrode shapes, sizes and gaps in between them according to the particle targeted in each case; particles can range from blood cells to molecules. The different arrays can be electrically independent and may be polarized with different signals. The goal of this system is to enable cell trapping and purification, their lysis and subsequent concentration of extracted molecules and organelles all in one device. Such device can then provide ideal working samples for analytical techniques such as PCR and DNA arrays. Such system could significantly decrease the cost and time of common diagnostic assays in clinical and environmental applications.

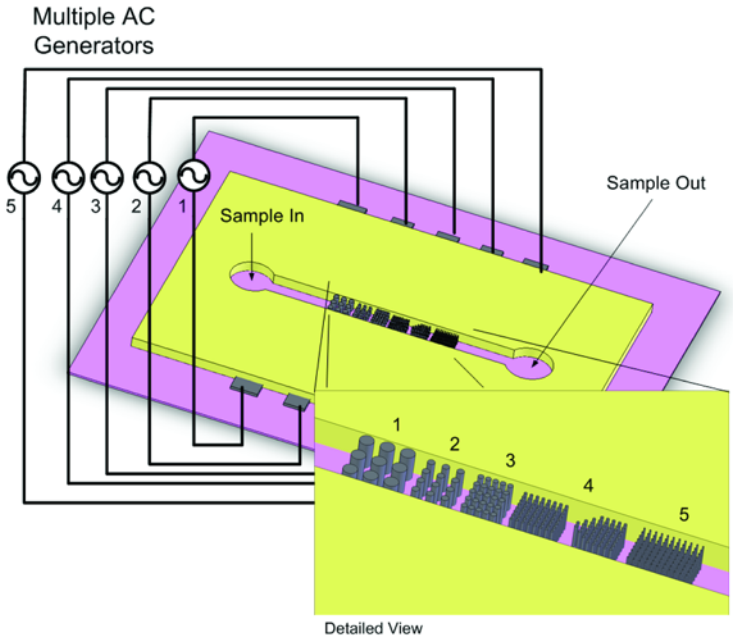

Figure 6. Schematic of a multi-stage carbonDEP device. A number of electrode arrays are embedded in a channel, each of such arrays are electrically independent allowing for their polarization using different electrical signals. From (33).

Acknowledgments

The author acknowledges collaboration with Prof. Juarez and Torrents at the Institute of Bioengineering of Catalonia; Prof. McKinney and Renaud, as well as Dr. Elitas, from Ecole Polytechnique Federale de Lausanne (EPFL); and Prof. Alexandra Ros and Dr. Camacho-Alanis from Arizona State University.

References

1. R. Martinez-Duarte, Electrophoresis, **33**, 3110-3132 (2012).
2. C. Wang, G. Jia, L. H. Taherabadi and M. J. Madou, J Microelectromech S, **14**, 348-358 (2005).
3. T. Shigemitsu and G. Matsumoto, Med & Biol Eng & Comput, **17**, 470 (1979).
4. B. Y. Park, L. Taherabadi, C. Wang, J. Zoval and M. J. Madou, J Electrochem Soc, **152**, J136-J143 (2005).
5. G. Turon Teixidor, R. A. Gorkin III, P. P. Tripathi, G. S. Bisht, M. Kulkarni, T. K. Maiti, T. K. Battacharyya, J. R. Subramaniam, A. Sharma, B. Y. Park and M. Madou, Biomed Mater, **3**, 034116 (2008).
6. J. Benson, J Biomed Mat Res, **5**, 41-47 (1971).
7. S. Yamada and H. Sato, Nature, **193**, 261-262 (1962).
8. F. C. Cowlard and J. C. Lewis, J Mat Sci, **2**, 507-512 (1967).
9. W. V. Kotlensky and H. E. Martens, Nature, **206**, 1246-1247 (1965).
10. G. M. Jenkins and K. Kawamura, Nature, **231**, 175-176 (1971).
11. M. C. Jaramillo, E. Torrents, R. Martinez-Duarte, M. Madou and A. Juarez, Electrophoresis, **31**, 2921-2928 (2010).
12. R. Martinez-Duarte, R. Gorkin, K. Abi-Samra, M. Madou, Lab-on-a-chip, **10** (8), 1030-1043 (2010).
13. R. Martinez-Duarte, S. Cito, E. Collado-Arredondo, S. O. Martinez and M. Madou, Sensors & Transducers Journal, **3**, 25-36 (2008).
14. T. B. Jones, IEEE Eng. Med. and Biol., **22**, 33-42 (2003).
15. R. Pethig, Biomicrofluidics, **4**, 022811-022846 (2010).
16. R. Martinez-Duarte, P. Renaud and M. J. Madou, Electrophoresis, **32**, 2385-2392 (2011).
17. R. Martinez-Duarte, Ph. D., University of California, Irvine (2010).
18. Alaeddini, R., Forensic Science International: Genetics, **6** (3), 297-305 (2012).
19. Radstrom, P., Knuttson, R. Wolffs, P., Dahlenborg, M., Lofstrom, C., Methods in Molecular Biology, **216**, 31-50 (2003).
20. Schriewer, A., Wehlmann, A., Wuertz, S., Journal of Microbiological Methods, **85** (1), 16-21 (2011).
21. Van Doorn, R., Klerks, M. M., van Gent-Pelzer, M. P., Speksnijder, A. G., Kowalchuk, G. A., Schoen, C. D., Applied and Environmental Microbiology, **75** (22), 7253-7260 (2009).
22. Rock, C., Alum, A., Abbaszadegan, M., Applied and Environmental Microbiology, **76** (24), 8102-8109 (2010).
23. M.C. Jaramillo, R. Martinez-Duarte, M. Hüttener, P. Renaud, E. Torrents and A. Juarez, Biosensors and Bioelectronics, **43**, 297-303 (2013).
24. Sagova-Mareckova, M., Cermak, L., Novotna, J., Plhackova, K., Forstova, J., Kopecky, J., Applied and Environmental Microbiology, **74** (9), 2902-2907 (2008).
25. J. W. Bigger, Lancet, **2**, 497-500 (1944).
26. N. Dhar, J. D. McKinney, Curr. Opin. Microbiol., **10**, 30-38 (2007).
27. M. Fauvart, V. N. De Groote, J. Michiels, J. Med. Microbiol., **60**, 699-709 (2011).

A. F. Altelaar, J. Munoz, A. J. R. Heck, Nat. Rev. Genet., **14**, 35-48 (2013).

28. H. Stower, Nat. Rev. Genet., **14**, 596-596 (2013).
29. M. Elitas, R. Martinez-Duarte, N. Dhar, J. D. McKinney, and P. Renaud, Lab-on-a-chip, submitted (2014)

30. R. Martinez-Duarte, F. Camacho-Alanis, P. Renaud and A. Ros, Electrophoresis, **34**, 1113-1122 (2013).
31. G. Mernier, R. Martinez-Duarte, R. Lehal, F. Radtke and P. Renaud, Micromachines, **3**, 574-581 (2012).
32. R. Martinez-Duarte, J. Andrade-Roman, S. O. Martinez and M. Madou, in Proceedings of NSTI-Nanotech: Boston, **3**, 316-319 (2008).